

The oxygen-helium ion transition level during low solar activity: II. A new empirical model

S. M. Stankov

Geophysical Institute, Bulgarian Academy of Sciences, Sofia 1113, Bulgaria

Abstract. A new empirical model of the O^+ - He^+ ion transition level during low solar activity is developed using *in-situ* measurements from the Atmosphere Explorer - C satellite. It simulates the level's longitudinal, latitudinal, seasonal and diurnal variations.

Keywords: transition level, satellite measurements, empirical modelling

1. Introduction

The O^+ - He^+ transition height (level) is one of the characteristic parameters of the ionospheric plasma. Therefore, the knowledge of this height is useful for a better understanding of the underlying chemical and transport processes, ionospheric storms, ion composition, etc. It could also serve as a reference when constructing and verifying ionospheric models (Bilitza, 1991). In the preceding companion paper (Stankov, 1999) the O^+ - He^+ transition height behaviour has been analysed leading to the following major conclusions: (a) the International Reference Ionosphere (IRI) model (Bilitza et al., 1993) is unsatisfactory for purposes of calculating the ion composition and the ion transition heights in particular; (b) the available direct encounters of the O^+ - He^+ transition level are insufficient to fully examine its behaviour under all spatial and temporal conditions; (c) a study of averaged altitude profiles of the individual ions provides additional helpful information; (d) a deeper study is required for reliably simulating the complex longitudinal and diurnal behaviour of the transition level.

The purpose of this paper is to present a new O⁺ - He⁺ transition height model for low solar activity, capable of simulating the level's longitudinal, latitudinal, seasonal and diurnal variations.

First, an additional analysis of the level's longitudinal and diurnal behaviour is provided, supplementing the previous study (Stankov, 1999). Second, the model's data base is built on a set of pre-defined geophysical parameters. Next, an approximation formula for a convenient calculation of the level is constructed. Finally, some exemplary model calculations are presented.

2. Data base

The O⁺- He⁺ transition height model's data base will be constructed using direct observations of the level and averaged ion density profiles both obtained from the Atmosphere Explorer - C (AE-C) satellite measurements.

Geophysical parameters

Considering the analysis of the transition level behaviour and the data availability, the required set of parameters for the model is: solar activity, season (month), local time, geomagnetic longitude, and geomagnetic latitude. Each parameter, its limits and optimal discretization are summarized in Table 1.

PARAMETER	unit	lower limit	upper limit	step size
SOLAR ACTIVITY	F10.7	80	240	-
SEASON	month	1	12	3
LOCAL TIME	hour	0	24	2
GEOM. LONGITUDE	degree	0	360	60
GEOM. LATITUDE	degree	-60	+60	10

Table 1. The geophysical parameters of the model.

The model covers low solar activity conditions only - the average observed value of the 10.7 cm (2800 MHz) solar radio flux is F10.7 = 85. The annual variations are represented by three seasons - winter, equinox, and summer. At this stage, no difference is made between the spring and autumn equinoxes. The latitudinal variations of the level have been described in detail (Stankov, 1999) but more research is required to better understand the longitudinal and diurnal variations.

Longitudinal variations

The scarcity of direct observations of the transition level, especially in the day-time, causes difficulties that can be alleviated by using averaged ion density profiles. The averaged altitude profiles are obtained after sorting all data into six longitude sections 0-60°, 60-120°, ... , 240-300°, 300-360°. Three latitude bands are separately researched: equatorial latitudes [-20°, +20°], middle latitudes [-40°, -20°]∪[+20°, +40°], and high latitudes [-60°, -40°]∪[+40°, +60°]. In addition, data from all latitudes [-60°, +60°] are collected. On the one hand, the ‘all-latitude’ data may provide information about the general pattern; on the other hand, these data help to determine the significance of a particular value and / or conclusion and help the statistical analysis in general. Day-time and night-time conditions are investigated; extrapolated values are not taken into account.

The *night-time* longitudinal behaviour of the transition level, as obtained from averaged ion density profiles, is presented in Fig.1. The local time windows are set to 1800-0600LT for winter, 1900-0500LT for equinox, and 2000-0400LT for summer conditions respectively. During summer (Fig.1, top panel), the majority of available data is for middle latitudes; limited equatorial data in the 120-240° longitude section exist too. Both patterns reveal broad minima at 240° longitude. The equatorial data also suggest a relatively large longitudinal variability of about 300 km. Far more data are available for equinox (Fig.1, middle panel). Again, the variability at low latitudes is significant - values ranging from 700 up to 1000 km. Limited high-latitude data exist for winter conditions (Fig.1, bottom panel); the available information implies that the variability in longitude direction is comparable in strength with the variability in latitude direction.

The *day-time* longitudinal behaviour of the transition level is given in Fig.2. The local time windows are now set to 0800-1600LT for winter, 0800-1700LT for equinox, and 0800-1800LT for summer. During the summer (Fig.2, top panel), most of the AE-C measurements are well below the O⁺- He⁺ transition height and extrapolation of the ion density profiles is necessary. Such an extrapolation is not considered in this study and it is possible to deduce only a limited number of values after collecting measurements from all latitudes. A closer look at the individual ion densities reveals a decrease of the level in the 120-240° longitude part and two factors are responsible for this. First, the oxygen ion density exhibits negligible changes at different longitudes. Second, the helium ion density (between 1200 and 1800 km height) is generally higher in the longitude section 120-240° than at other longitudes. Hence, the level in this longitude region should be lower (about 10-20%) than elsewhere. More data exist about equinox (Fig.2, middle panel) and winter (Fig.2, bottom panel). Generally, the day-time

longitudinal behaviour is more complicated than the night-time behaviour. Several local minima are observed particularly at low and equatorial latitudes suggesting interaction of many processes and factors. Also, the variability in longitude direction is relatively smaller than in latitude direction.

The focus of this study is on the longitudinal variations using averaged ion density profiles; the mean value in a given latitude band can be compared with the corresponding value obtained by the same method applied when investigating the latitudinal variations (Stankov, 1999). A comparison has been made and consequently differences revealed due to the following factors:

a) Enlarged local-time windows, e.g. during winter the data are collected from a significantly wider time interval 1800-0600 LT.

b) Nature of the diurnal variations, e.g. the local time of the transition level's minimum is varying within a pre-dawn period of up to two hours and the minimum is certainly not observed at midnight.

c) Limited number of data available in some cases, particularly during the day.

d) Inaccuracy of the ion density profiles extrapolation.

Some discrepancies are also observed between the transition level's values deduced from averaged ion density profiles and the values directly encountered by the satellite. Factors that may cause these discrepancies are:

a) Nature of the averaging process in altitude direction when obtaining density height profiles. In some cases (due to limited data) the averaging is over 100 km, which may induce uncertainty of several tens of kilometers; the direct measurements of the level cause no such problem.

b) Existence of the so-called 'density tolerance' when obtaining the direct encounters of the level. This tolerance (no matter how small it is) may lead to significant errors especially when the proximity of the O⁺ and He⁺ densities lasts for an extended height interval. Then, 'direct encounters' will be recorded along the whole altitude interval - the averaging of these encounters may not necessarily indicate the correct level.

c) Existence of data gaps in the altitude distribution of the ion densities. If a correct TL is within the altitude range of this gap, the 'direct' method may still record some encounters outside the gap; using the 'average' method will certainly point to a value within the altitude range of the gap.

d) Limited data in some temporal and / or spatial intervals.

e) Large data scattering.

In different situations different factors dominate over the others and the combined effect may be quite difficult to analyse.

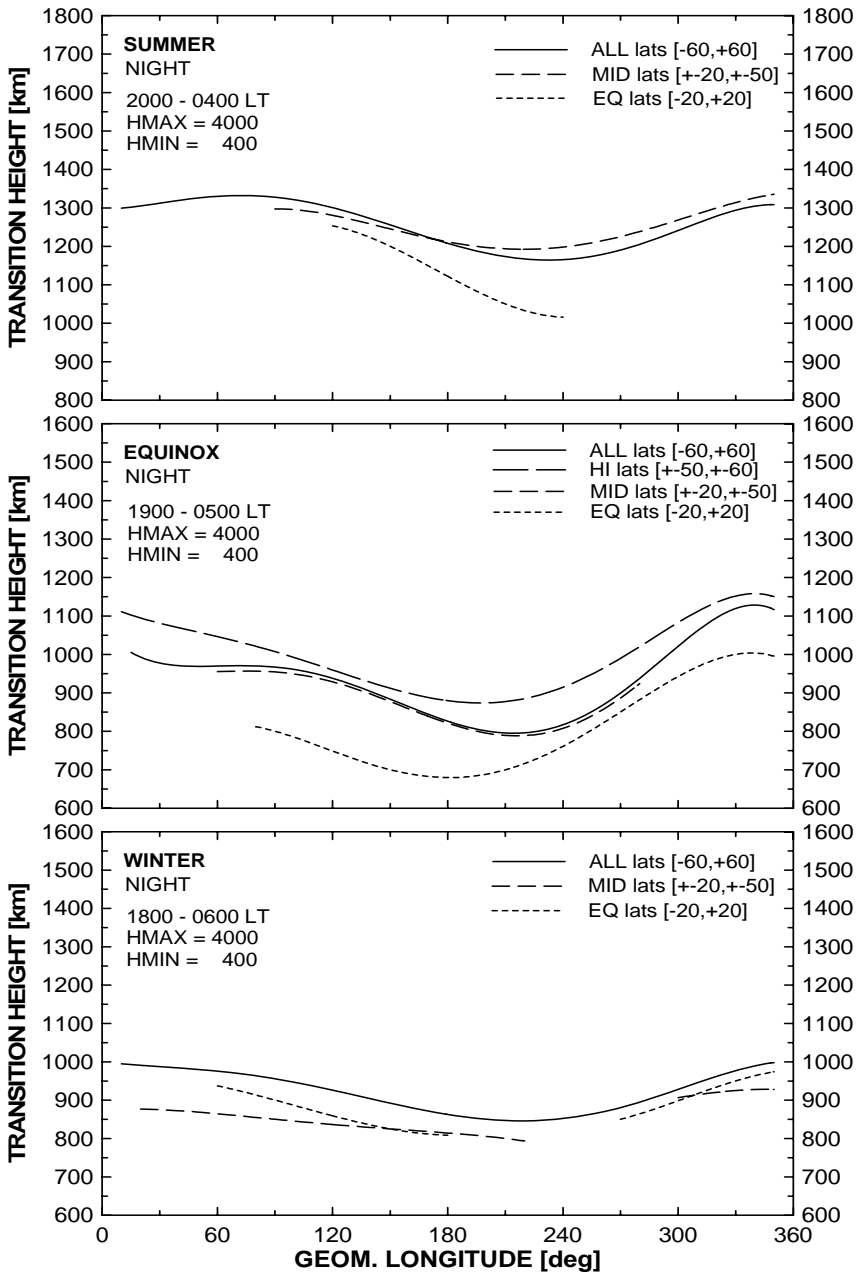


Fig.1 Longitudinal variations of the *night-time* O^+ - He^+ transition level as deduced from averaged ion density profiles. HMIN and HMAX indicate the height limits over which the data were taken.

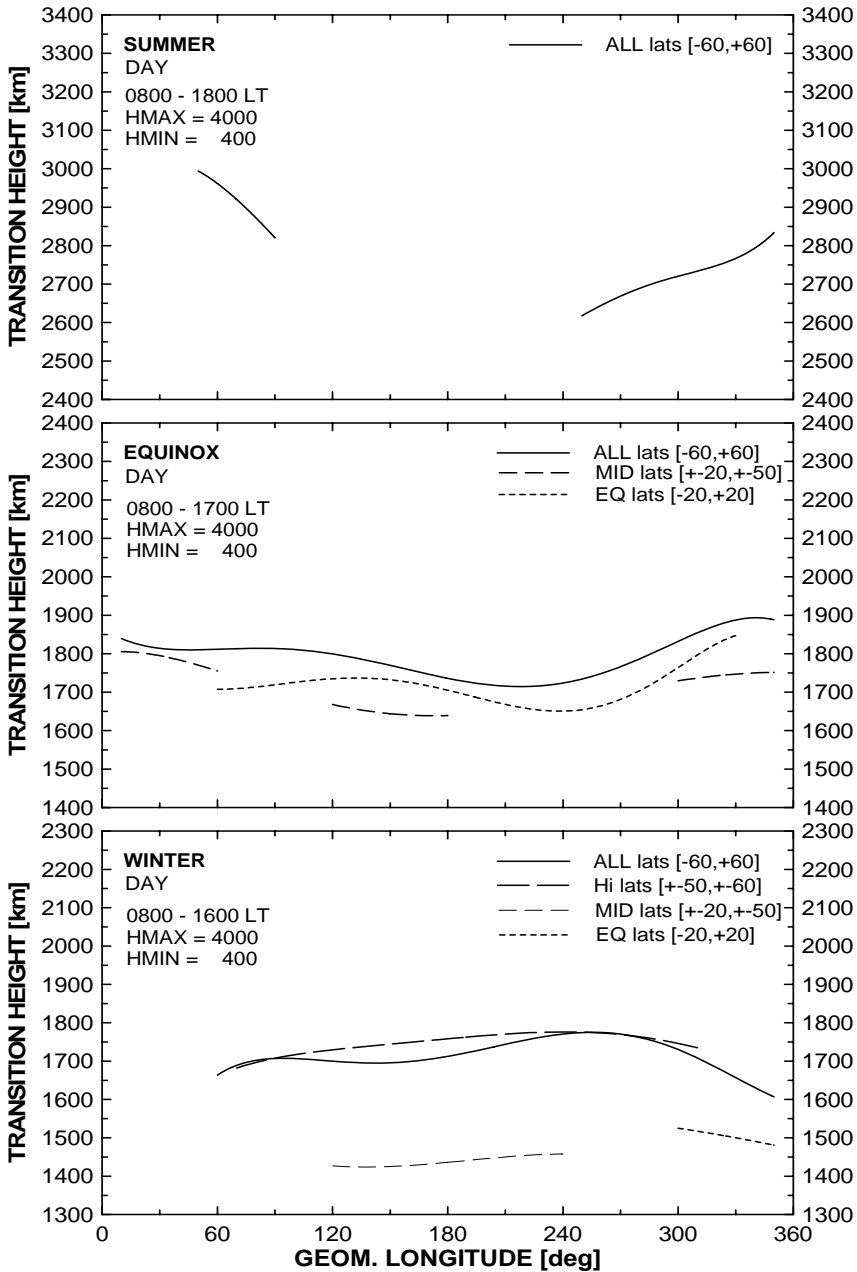


Fig.2 Longitudinal variations of the *day-time* O^+ - He^+ transition level as deduced from averaged ion density profiles. HMIN and HMAX indicate the height limits over which the data were taken.

The next step in building the model's data base is the reconstruction of the longitudinal behaviour. First, the approximation set is built following the discretization scheme (Table 1) of the geophysical parameters. The approximation set is denoted $\{(i, j) ; i, j = 1, 2, \dots, 6\}$, where i is the 'longitude' index $i = 1$ [0-60°], 2 [60-120°], ... , 6 [300-360°] and j is the 'latitude' index $j = 1$ [0-10°], 2 [10-20°], ... , 6 [50-60°]. The aim is to obtain the value y_{ij} of the transition level at its corresponding set point (i, j) by using both average density profiles and TL direct measurements data that have been derived so far. The idea is to start from the average value a_j (the transition level value deduced from the density profile for a given j -th latitude band (refer to Table 2 and Table 3, (Stankov, 1999))) and to 'spread' this value over the whole longitude range 0-360° using the obtained pattern of longitudinal behaviour. The average a_j is assumed to be the most important and reliable value. The following formula is constructed for calculation of the transition level, y_{ij} , at a given set point:

$$y_{ij} = \delta_{1j} a_j + (1 - \delta_{1j}) r_{aj} + \left(\frac{x_{ij}^{(p)} - x_{mj}^{(p)}}{x_{mj}^{(p)}} \right) \left(\frac{r_{mj}^{(d)}}{r_{mj}^{(p)}} \right) a_j, \quad i = 1, 2, \dots, 6 \quad j = 1, 2, \dots, 6$$

where $\delta_{1j} \in [0, 1]$ and

$$x_{mj}^{(*)} = \frac{1}{n_i} \sum_{i=1}^{n_i} x_{ij}^{(*)}, \quad j = 1, 2, \dots, 6$$

$$r_{mj}^{(*)} = \max_i \left\{ x_{ij}^{(*)} \right\} - \min_i \left\{ x_{ij}^{(*)} \right\}, \quad j = 1, 2, \dots, 6$$

$$r_{aj} = \delta_{2j} x_{mj}^{(p)} + (1 - \delta_{2j}) x_{mj}^{(d)}, \quad \delta_{2j} \in [0, 1], \quad j = 1, 2, \dots, 6$$

and x_{ij} is the transition level at a set point (i, j) obtained from 'direct measurement' (superscript ^(d)) and 'density profile' (superscript ^(p)) respectively; the mean value for a given j -th latitude band is denoted by x_{mj} .

The reason of applying the factors R_j , r_{aj} , and δ_{1j} have been discussed above: the 'amplitude corrector' $R_j (= r^{(p)} / r^{(d)})$ and 'average corrector' r_{aj} exist to reconcile the different ways of deducing the level - direct and profile; the other factor δ_{1j} is used to minimise the error of using extrapolation when deducing values by the 'average profile' method.

The calculated spatial variations of the O⁺- He⁺ transition level are presented in Table 2; it is assumed that $\delta_{1j} = 1$ and $R_j = 1$.

long lat	0 - 60	60 - 120	120 - 180	180 - 240	240 - 300	300 - 360	0 - 60	60 - 120	120 - 180	180 - 240	240 - 300	300 - 360
-------------	--------	-------------	--------------	--------------	--------------	--------------	--------	-------------	--------------	--------------	--------------	--------------

	<i>summer : night-time</i>						<i>summer : day-time</i>					
50-60	1452	1474	1392	1302	1336	1446	3774	3536	3332	3230	3366	3536
40-50	1186	1240	1193	1135	1174	1273	3465	3432	3234	3135	3267	3432
30-40	1186	1240	1193	1135	1174	1273	3150	3120	2940	2850	2970	3120
20-30	1087	1136	1093	1041	1076	1167	3150	3120	2940	2850	2970	3120
10-20	945	1190	1120	980	1120	1080	2940	2912	2744	2660	2772	2912
0 - 10	1080	1360	1280	1120	1280	1080	2520	2496	2352	2280	2376	2496
-10 - 0	1080	1360	1280	1120	1280	1080	2520	2496	2352	2280	2376	2496
-20-10	945	1190	1120	980	1120	1080	2940	2912	2744	2660	2772	2912
-30-20	1087	1136	1093	1041	1076	1167	3150	3120	2940	2850	2970	3120
-40-30	1186	1240	1193	1135	1174	1273	3150	3120	2940	2850	2970	3120
-50-40	1186	1240	1193	1135	1174	1273	3465	3432	3234	3135	3267	3432
-60-50	1452	1474	1392	1302	1336	1446	3774	3536	3332	3230	3366	3536

	<i>equinox : night-time</i>						<i>equinox : day-time</i>					
50-60	1186	1100	992	967	1096	1259	2424	2448	2328	2280	2352	2520
40-50	1025	957	897	807	906	1109	2319	2189	2125	2134	2189	2244
30-40	971	906	850	764	859	1050	2108	1990	1932	1940	1990	2040
20-30	917	856	802	722	811	992	1950	1841	1787	1795	1841	1887
10-20	927	825	721	722	876	1030	1716	1675	1699	1621	1665	1818
0 - 10	1146	1019	890	892	1082	1272	1718	1677	1701	1623	1667	1820
-10 - 0	1146	1019	890	892	1082	1272	1718	1677	1701	1623	1667	1820
-20-10	927	825	721	722	876	1030	1716	1675	1699	1621	1665	1818
-30-20	917	856	802	722	811	992	1950	1841	1787	1795	1841	1887
-40-30	971	906	850	764	859	1050	2108	1990	1932	1940	1990	2040
-50-40	1025	957	897	807	906	1109	2319	2189	2125	2134	2189	2244
-60-50	1186	1100	992	967	1096	1259	2424	2448	2328	2280	2352	2520

	<i>winter : night-time</i>						<i>winter : day-time</i>					
50-60	1010	980	924	873	911	1001	1727	1715	1767	1785	1790	1715
40-50	883	859	817	812	846	883	1484	1493	1485	1535	1557	1448
30-40	831	809	769	764	796	831	1335	1343	1337	1381	1401	1303
20-30	883	859	817	812	846	883	1286	1294	1287	1330	1349	1255
10-20	1050	950	823	752	850	975	1236	1244	1238	1279	1298	1206
0 - 10	1109	1003	868	794	897	1029	1212	1219	1213	1253	1272	1182
-10 - 0	1109	1003	868	794	897	1029	1212	1219	1213	1253	1272	1182
-20-10	1050	950	823	752	850	975	1236	1244	1238	1279	1298	1206
-30-20	883	859	817	812	846	883	1286	1294	1287	1330	1349	1255
-40-30	831	809	769	764	796	831	1335	1343	1337	1381	1401	1303
-50-40	883	859	817	812	846	883	1484	1493	1485	1535	1557	1448
-60-50	1010	980	924	873	911	1001	1727	1715	1765	1785	1790	1715

Table 2. The $O^+ - He^+$ transition height model's data base: night-time (left side) and day-time (right side) values [km] for summer (top), equinox (middle), and winter (bottom) seasons.

Diurnal variations

Preliminary results of the diurnal behaviour have already been obtained (Stankov, 1999). They are incomplete because only average night-time and day-time conditions have been considered. A more detailed analysis is required to cover the complex sunrise and sunset periods of fast changes.

The AE-C satellite measurements of ion densities are sorted again according to local time only - no spatial variations are taken into account. The optimal discretisation step is found to be two hours; longer periods are too big to describe the dawn and dusk periods, shorter periods contain an insufficient number of measurements. The 'direct measurement' and 'average ion density profile' methods are applied again.

Following the definition of the 'direct measurement' (Stankov, 1999), the transition level can be measured with different precision, ε_{dens} , with respect to ion density. In the night-time, $\varepsilon_{dens} = 0.01$ secures good enough precision to determine the level reliably but it is definitely insufficient during the day. That is why two different extracts have been made; with $\varepsilon_{dens} = 0.01$ (closed circles) and $\varepsilon_{dens} = 0.05$ (open circles). The scattering is larger when $\varepsilon_{dens} = 0.05$ but the differences between the average values are small.

During summer (Fig.3, top panel) information about the transition level is obtained for the dusk and evening period 1600 - 2400 LT only. The averages drop from 1800 km down to about 1000-1100 km at midnight.

During equinox (Fig.3, middle panel), the measurements are in abundance. The transition level at midnight is in the 900-950 km interval, decreases to its diurnal minimum observed in the pre-dawn period 0400-0600 LT and then starts increasing in the morning hours. After reaching its maximum around noon, the level starts decreasing again in the afternoon hours. The data scattering around noon (1000 - 1600 LT) is quite large for $\varepsilon_{dens} = 0.05$. This is probably due to the ion-ion drag leading to unusually high concentrations of O⁺ preserved well above the transition height. The noon maximum derived from ion density profiles is 1900 km, which is significantly lower than the maximum obtained by the other method.

During winter (Fig.3, bottom panel), the level's behaviour is similar to that during equinox. However, the afternoon decrease of the level during winter is faster than the corresponding decreases during equinox and summer. Also, the averages obtained by direct measurements of the level are substantially lower than the values deduced from ion density profiles.

The next task is to apply the obtained pattern of diurnal changes to the day-time and night-time values (Table 2) in order to construct a time-dependent data base.

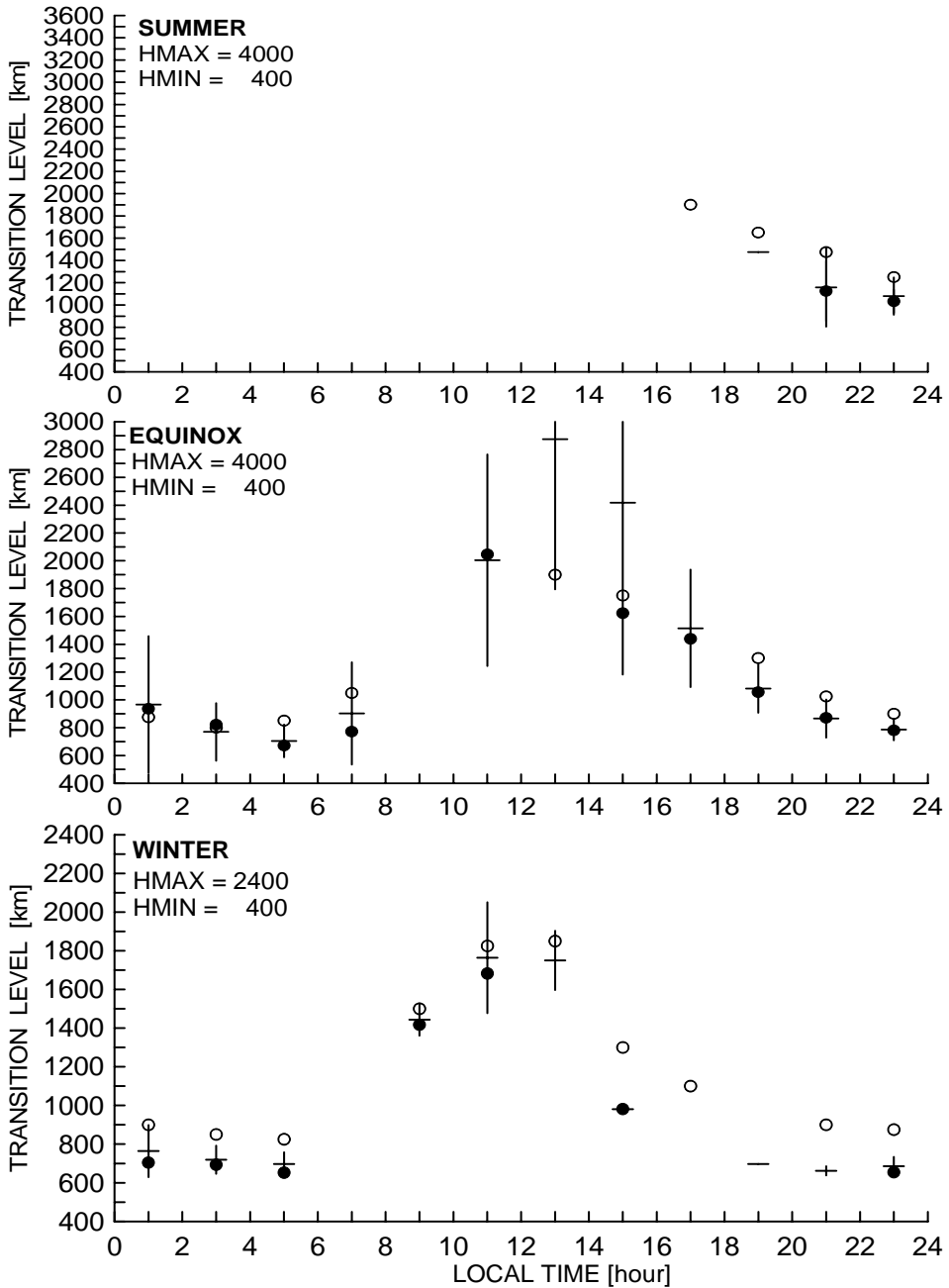


Fig.3 Diurnal variations of the $O^+ - He^+$ transition level as measured by AE-C satellite. HMIN and HMAX indicate the height limits over which the data were taken. Direct encounters are obtained with density tolerance $\epsilon_{dens} = 0.01$ (closed circles) and $\epsilon_{dens} = 0.05$ (crosses); the crosses include the standard deviations (vertical bars) and the averages (horizontal bars). The open circles indicate the values deduced from averaged ion density profiles.

The analysis made so far suggests that the combined use of trigonometric and parabolic approximations is appropriate for representing the diurnal behaviour of the O^+ - He^+ transition level; the day-time variations are treated separately from the night-time variations.

The following function is proposed here to simulate the day-time behaviour, i.e. for $t \in [t_{dawn} - \tau_{pre}, t_{dusk}]$:

$$f_d(t) = f(t_{\min}) + 0.5[f(t_{\max}) - f(t_{\min})] \left\{ 1 + \sin \left[\frac{2\pi}{T} (t - \varphi) \right] \right\}$$

where the period T and phase φ are defined as follows

$$T = 2(t_{\max} - t_{\min})$$

$$\varphi = 0.5(t_{\max} + t_{\min})$$

and

$$t_{\min} = t_{dawn} - \tau_{pre}$$

$$t_{\max} = 0.5(t_{dawn} + t_{dusk})$$

The local time of dawn is denoted by t_{dawn} and the time of dusk by t_{dusk} . The parameter τ_{pre} provides the length of the predawn period ($t_{dawn} - \tau_{pre}, t_{dawn}$); the length is estimated to vary between 1.5 and 2.0 hours (see Fig.3) depending on season and latitude. It is exactly in this predawn interval when the transition level's minimum is observed.

The night-time level, i.e. for $t \in (t_{dusk}, t_{dawn} - \tau_{pre})$, is calculated by:

$$f_n(t) = f(t_{\min}) + \frac{[f(t_{\max}) - f(t_{\min})]}{(t_{\max} - t_{\min})^2} (t - t_{\max})^2$$

where

$$t_{\min} = t_{dawn} - \tau_{pre}$$

$$t_{\max} = t_{dusk}$$

The local times of sunrise and sunset are calculated by functions used in the IRI model. It is also possible to include the sunrise and sunset times in a simpler function of the solar zenith angle, as for example is done in other empirical studies on the transition levels (Miyazaki, 1979).

The proposed formulae are applied on the average values of the level (Stankov, 1999) to obtain the diurnal variations for each latitude band. The results are provided in Table 3.

LT lat	0-2	2-4	4-6	6-8	8-10	10-12	12-14	14-16	16-18	18-20	20-22	22-24
-----------	-----	-----	-----	-----	------	-------	-------	-------	-------	-------	-------	-------

summer

50-60	1440	1407	1513	1954	2596	3169	3431	3271	2757	2105	1655	1517
40-50	1243	1210	1305	1752	2419	3020	3295	3127	2587	1908	1448	1316
30-40	1238	1211	1281	1656	2232	2755	2996	2849	2378	1791	1400	1295
20-30	1147	1108	1177	1563	2174	2735	2994	2835	2330	1705	1346	1227
10-20	1115	1081	1135	1478	2036	2554	2794	2647	2180	1606	1284	1182
0-10	1229	1207	1239	1471	1862	2228	2399	2295	1963	1560	1339	1273
-10-0	1229	1207	1239	1471	1862	2228	2399	2295	1963	1560	1339	1273
-20-10	1115	1081	1135	1478	2036	2554	2794	2647	2180	1606	1284	1182
-30-20	1147	1108	1177	1563	2174	2735	2994	2835	2330	1705	1346	1227
-40-30	1238	1211	1281	1656	2232	2755	2996	2849	2378	1791	1400	1295
-50-40	1243	1210	1305	1752	2419	3020	3295	3127	2587	1908	1448	1316
-60-50	1440	1407	1513	1954	2596	3169	3431	3271	2757	2105	1655	1517

equinox

50-60	1138	1112	1103	1237	1652	2125	2363	2216	1777	1355	1233	1178
40-50	987	962	954	1082	1484	1942	2172	2029	1605	1196	1078	1025
30-40	932	911	903	1017	1370	1773	1975	1850	1477	1117	1013	966
20-30	879	860	853	956	1277	1644	1827	1714	1374	1047	953	910
10-20	875	858	853	940	1213	1524	1680	1584	1295	1017	937	901
0-10	1069	1056	1051	1119	1328	1567	1686	1613	1391	1178	1117	1089
-10-0	1069	1056	1051	1119	1328	1567	1686	1613	1391	1178	1117	1089
-20-10	875	858	853	940	1213	1524	1680	1584	1295	1017	937	901
-30-20	879	860	853	956	1277	1644	1827	1714	1374	1047	953	910
-40-30	932	911	903	1017	1370	1773	1975	1850	1477	1117	1013	966
-50-40	987	962	954	1082	1484	1942	2172	2029	1605	1196	1078	1025
-60-50	1138	1112	1103	1237	1652	2125	2363	2216	1777	1355	1233	1178

winter

50-60	991	969	957	973	1190	1551	1725	1551	1228	1118	1066	1024
40-50	884	865	854	871	1054	1343	1480	1343	1084	993	948	912
30-40	829	812	803	820	980	1221	1334	1221	1005	927	887	854
20-30	871	861	856	870	1003	1197	1287	1197	1009	929	905	885
10-20	1011	1005	1002	1012	1088	1194	1243	1194	1092	1046	1032	1020
0-10	1106	1102	1101	1107	1146	1198	1222	1198	1147	1124	1117	1110
-10-0	1106	1102	1101	1107	1146	1198	1222	1198	1147	1124	1117	1110
-20-10	1011	1005	1002	1012	1088	1194	1243	1194	1092	1046	1032	1020
-30-20	871	861	856	870	1003	1197	1287	1197	1009	929	905	885
-40-30	829	812	803	820	980	1221	1334	1221	1005	927	887	854
-50-40	884	865	854	871	1054	1343	1480	1343	1084	993	948	912
-60-50	991	969	957	973	1190	1551	1725	1551	1228	1118	1066	1024

Table 3. The O^+ - He^+ transition height model's data base: diurnal variations (on the average value for all longitudes); summer values are on the top, equinox - in the middle, winter - at the bottom.

3. Approximation formula

The O^+ - He^+ transition level is approximated by a multi-variable polynomial, which has the following form

$$P(C, N; X) = \sum_I C(I).G(I, X) =$$

$$= \sum_{i_1=1}^{n_1} \sum_{i_2=1}^{n_2} \sum_{i_3=1}^{n_3} \sum_{i_4=1}^{n_4} \sum_{i_5=1}^{n_5} C(i_1, i_2, \dots, i_5) \cdot g_1(i_1, x_1) \cdot g_2(i_2, x_2) \dots g_5(i_5, x_5)$$

where

$$C(I) = C(i_1, i_2, \dots, i_5) \quad \text{- coefficients}$$

$$G(I, X) = g_1(i_1, x_1) \cdot g_2(i_2, x_2) \dots g_5(i_5, x_5) \quad \text{- generalised basis function}$$

$$N = (n_1, n_2, \dots, n_5) \quad \text{- number of basis functions}$$

$$I = (i_1, i_2, \dots, i_5), \quad i_m = 1, 2, \dots, n_m; \quad m = 1, 2, \dots, 5 \quad \text{- indices}$$

$$X = \prod_{m=1}^5 [x_L^{(m)}, x_R^{(m)}], \quad x \in X \subset \mathfrak{R}^5 \quad \text{- variables}$$

The set

$$\{g_m(i_m, x_m)\}_{i_m=1}^{n_m}$$

is a system of linearly independent functions on the domain of the m^{th} parameter. Any of the following orthogonal systems can be used:

$$1, x, x^2, \dots, x^{n_m} \quad \text{- algebraic basis}$$

$$1, \sin x, \cos x, \dots, \sin n_m x, \cos n_m x \quad \text{- trigonometric basis}$$

$$\cos(n \cdot \arccos x), \quad n = 1, 2, \dots, n_m \quad \text{- Chebyshev basis}$$

Each approximation has advantages and shortcomings (Dahlquist and Bjorck, 1974); the choice depends mainly on the type of variations induced by a particular geophysical parameter. Using the *algebraic* polynomials is a fast and easy way of approximating all types of the level variations securing high accuracy near the data points. The *trigonometric* approximation (Hildebrand, 1974) is very useful when approximating a periodic function. This set is orthogonal over any period interval and the derivative of each member is also a member. The *Chebyshev* polynomials (Berezin and Zhidkov, 1965) are orthogonal in the interval $[-1, 1]$ over a weight $(1-x^2)^{-1/2}$, and the approximation using these polynomials provides the smallest maximum deviation from the true function.

4. Numerical method for calculating the polynomial coefficients

The method of the least squares fit is applied for calculating the coefficients of the fitting polynomial (Hamming, 1962; Bevington, 1969; Gerald, 1970).

The model's data base (described above) is denoted by

$$\{x_n, y_n, p_n\}_{n=1}^{ND}$$

where $x_n = (x_{n1}, x_{n2}, \dots, x_{n5})$ is a data point ($x_n \in \mathbb{R}^5$), y_n is the value at x_n ($y_n \in \mathbb{R}^1$), p_n is the weight, ND is the number of data points.

A set of coefficients $\{C(I)\}_I$ is being sought, for which the functional

$$F(C) = \left\{ \sum_{n=1}^{ND} p_n (y_n - P(C, N; X))^2 \right\}^{1/2}$$

reaches its minimum. That means the following system should be solved:

$$\frac{dF}{dC_I} = 0 \quad , \quad I \in \mathbb{N}^5, \quad I \leq N$$

that is (in matrix form)

$$A(I, J).C(I) = B(I)$$

where

$$A(I, J) = \sum_{n=1}^{ND} p_n G(I, x_n) G(J, x_n)$$

$$B(I) = \sum_{n=1}^{ND} p_n G(I, x_n) y_n$$

$$I \in \mathbb{N}^5, \quad I \leq N, \quad 1 \leq i_m \leq n_m$$

$$J \in \mathbb{N}^5, \quad J \leq N, \quad 1 \leq j_m \leq n_m$$

Solving the equations simultaneously gives the required coefficients $C(I)$.

5. Exemplary model calculations

The model's data base presented here is constructed primarily from the AE-C measurements and is therefore much closer to the 'true' transition height values (Stankov, 1999) than the IRI model. The theoretical background of the proposed fit is discussed elsewhere (Bevington, 1969).

A detailed verification of the proposed model will be provided in a follow-on publication. Here, only some exemplary calculations of the constructed empirical model (using trigonometric approximation) are presented.

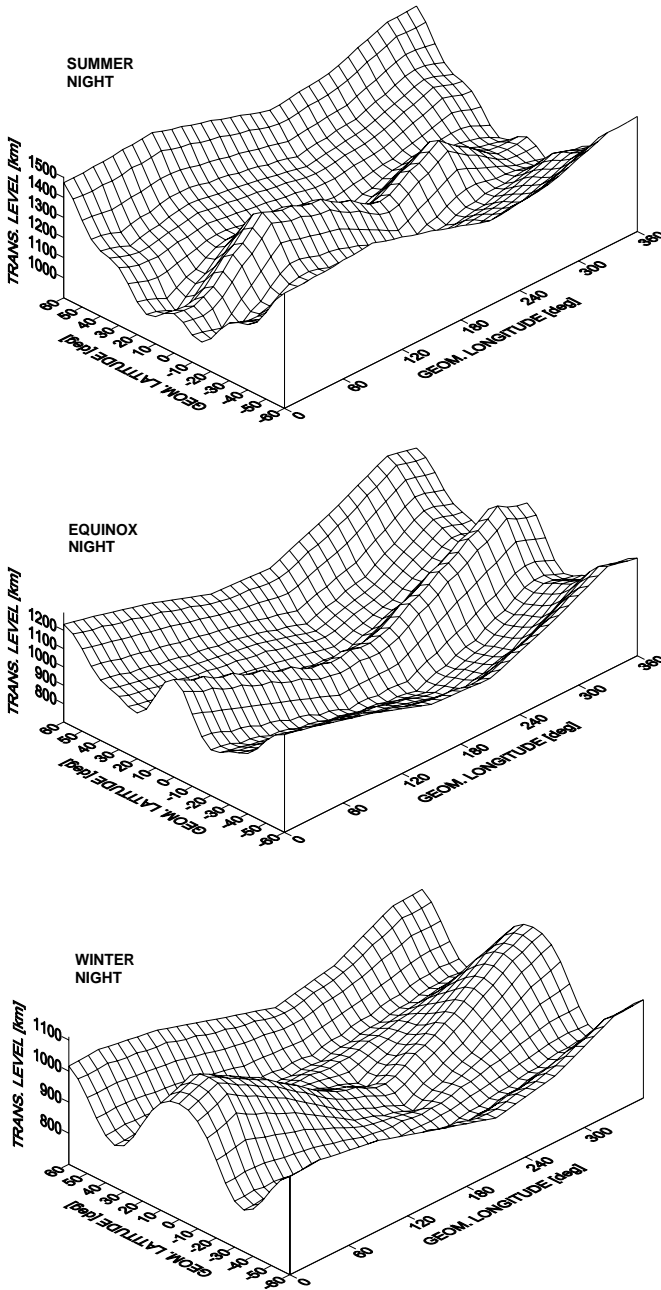


Fig.4 The simulated night-time $O^+ - He^+$ transition level for summer (top), equinox (middle), and winter (bottom). Surface plotted after gridding with radial basis functions; anisotropy ratio = 2.0 and angle = 0° .

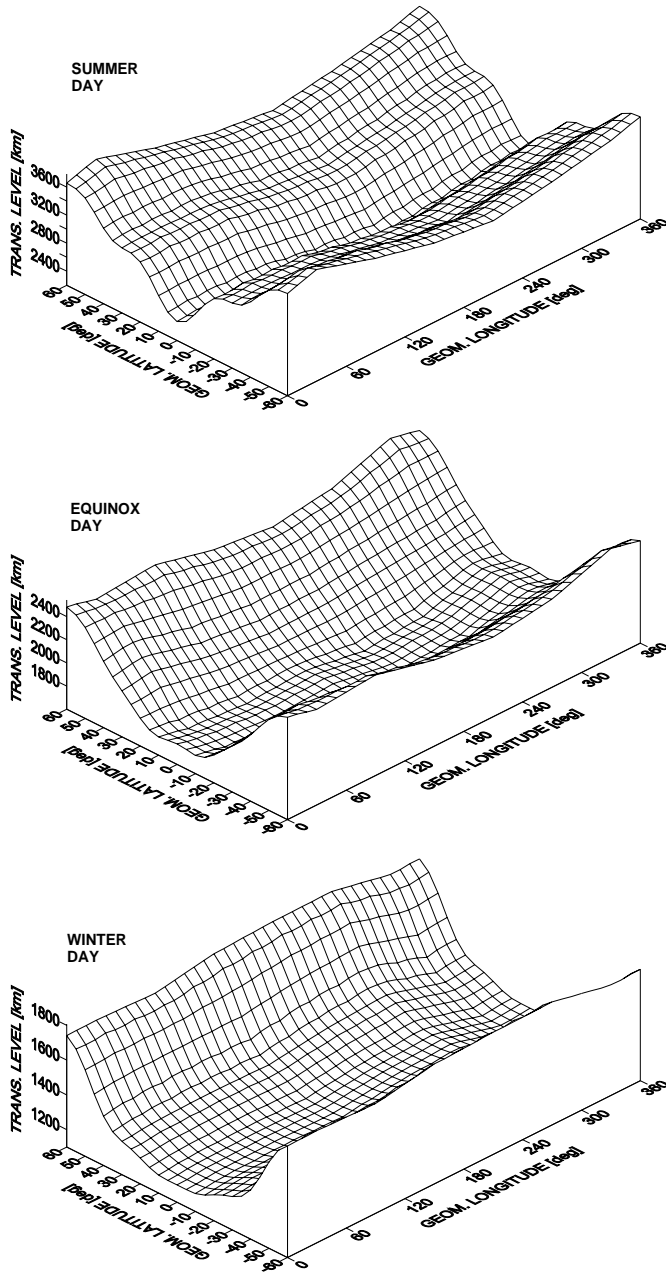


Fig.5 The simulated day-time O^+ - He^+ transition level for summer (top), equinox (middle), and winter (bottom). Surface plotted after gridding with radial basis functions; anisotropy ratio = 2.0 and angle = 0° .

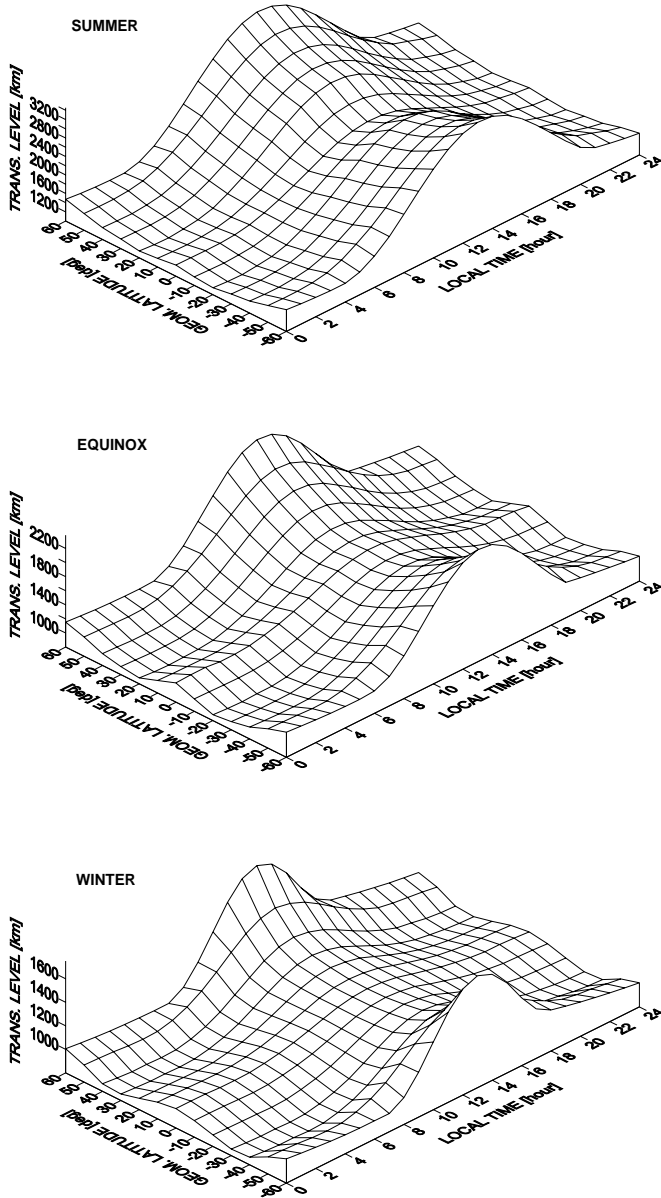


Fig.6 The simulated diurnal variations of $O^+ - He^+$ transition level for summer (top panel), equinox (middle panel), and winter (bottom panel) conditions.

The simulated *spatial* distribution of the ion transition height is presented in Fig.4 (night-time) and Fig.5 (day-time). The left-side oblique axis shows the geomagnetic latitude from -60° to $+60^{\circ}$, and the right-side oblique axis shows the geomagnetic longitude from 0° to 360° . The vertical axis shows the altitude in km (note the different scale for each season). As mentioned before, the differences in the ion density distribution between the hemispheres are not considered at this stage, so as a consequence there is symmetry of the transition height between the northern and southern hemispheres. In the night-time, the geomagnetic latitudinal variations are generally similar to each other, however the magnitudes of the changes are quite different particularly in the remarkable equatorial rise. This rise indicates either a large seasonal change in the proportion of neutral helium in the upper atmosphere or a steady flow of light ions from the summer to the winter hemisphere. A similar fact is recorded in the O⁺-H⁺ transition height behaviour (Titheridge, 1976).

The simulated *diurnal* behaviour of the O⁺-He⁺ transition height is provided in Fig.6 for summer (top panel), equinox (middle panel), and winter (bottom panel). The left-side oblique axis shows the geomagnetic latitude from -60° to $+60^{\circ}$, the right-side oblique axis shows the local time from 0000 to 2400 LT, and the vertical axis shows the altitude in km. During all three seasons, the ion transition level around the geomagnetic equator demonstrates a weak dependence on local time but is significantly stronger changing with local time at higher geomagnetic latitudes.

6. Conclusions

Using the IRI-95 (Danilov-95 ion composition option) the O⁺-He⁺ transition height has been calculated and compared with AE-C data (Stankov, 1999), revealing significant deviations of the IRI values from the real measurements. After a detailed analysis, AE-C satellite measurements have been used to construct a new empirical model of the O⁺-He⁺ transition level valid for low solar activity and three seasons - winter, equinox and summer. The diurnal variations are fully represented. The space covered is enclosed between geomagnetic latitudes -60° and $+60^{\circ}$ and all geomagnetic longitudes - from 0° to 360° ; further research is necessary to include the polar regions as well.

The simulation is much more reliable for night-time conditions when significantly more data have been used. Additional measurements are required to further understand and precisely represent the longitudinal behaviour. The sunrise and sunset periods, with the rapid changes of ion composition, need attention.

The constructed model is useful mainly in a computational context, providing convenience when referencing the level with respect to season, local time, longitude, and latitude. Another positive feature of the model is its analytical form. This allows an arbitrary choice of discretisation and easy evaluation of the level in regard to each geophysical parameter. Also, the model can be very easily expanded and corrected if more data or theoretical research become available. The approach proposed here can also be applied in other studies, e.g. for global parameterization based on theoretical models (Daniell et al., 1995).

Acknowledgments: The International Reference Ionosphere model and the Atmosphere Explorer measurement data were provided by the National Space Science Data Center through the World Data Center-A for Rockets and Satellites, Goddard Space Flight Center.

Topical Editor thanks N.Kilifarska and I.Kutiev for their help in evaluating this paper.

References

- Berezin I.S., and N.P.Zhidkov, 1965. *Computing methods*. Pergamon Press, Oxford.
- Bevington P.R., 1969. *Data reduction and error analysis for the physical sciences*. McGraw-Hill Book Co., New York.
- Bilitza D., 1991. The use of transition heights for the representation of ion composition. *Advances in Space Research* , **11**, No.10, (10)183-(10)186.
- Bilitza D., K.Rawer, L.Bossy, and T.Gulyaeva, 1993. International Reference Ionosphere - past, present and future: II. Plasma temperatures, ion composition and ion drift. *Advances in Space Research* , **13**, No.3, (3)15-(3)23.
- Dahlquist G., and A.Bjorck, 1974. *Numerical methods*. Prentice-Hall, Englewood Cliffs, N.J.
- Daniell R.E., L.D.Brown, D.N.Anderson, M.W.Fox, P.H.Doherty, D.T.Decker, J.J.Sojka, and R.W.Schunk, 1995. Parameterized ionospheric model: A global ionospheric parameterization based on first principles models. *Radio Science* , **30**, No.5, 1499-1510.
- Gerald C.F., 1970. *Applied numerical analysis*. Addison-Wesley Publ. Co., Reading, Massachusetts.
- Hamming R.W., 1962. *Numerical methods for scientists and engineers*. McGraw-Hill Book Co., New York.
- Hildebrand F.B., 1974. *Introduction to numerical analysis*. Dover Publications Inc., New York.
- Kutiev I., S.M.Stankov, and P.Marinov, 1994. Analytical expression of O⁺- H⁺ transition surface for use in IRI. *Advances in Space Research* , **14**, No.12, (12)135-(12)138.
- Mandel J., 1964. *The statistical analysis of experimental data*. Dover Publications Inc., New York.
- Miyazaki S., 1979. Ion transition height distribution obtained with the satellite TAIYO. *Journal of Geomagnetism and Geoelectricity* , **31**, Supplement, S113-S124.
- Stankov S.M., 1999. The oxygen-helium ion transition level during low solar activity: I. Comparison of AE-C satellite data with IRI model calculations. *Bulgarian Geophysical Journal* , **25**, No.1-4, 95-116.
- Titheridge J.E., 1976. Ion transition heights from topside electron density profiles. *Planetary and Space Science* , **24**, 229-245.

Преходното O^+ - He^+ ниво по време на ниска слънчева активност: II. Нов емпиричен модел

С. М. Станков

Резюме. Разработен е нов емпиричен модел на преходното O^+ - He^+ ниво по време на ниска слънчева активност с използване на *in-situ* измервания от спътника Atmosphere Explorer - C. Моделират се дължинните, ширинните, сезонните и денонощните вариации.

Първо, направен е допълнителен анализ на дължинните и денонощните вариации на преходното ниво. Второ, конструира се база данни върху предварително дефинираните геофизични параметри. След това се предлага аналитична формула за удобно пресмятане на преходната височина. Накрая са изложени моделни пресмятания на част от пространствените и времевите изменения на нивото.